Nature of Hydrogen Transfer in Soybean Lipoxygenase 1: Separation of Primary and Secondary Isotope Effects†

Keith W. Rickert and Judith P. Klinman*

Department of Chemistry, University of California, Berkeley, California 94720

Received April 9, 1999

ABSTRACT: Previous measurements of the kinetics of oxidation of linoleic acid by soybean lipoxygenase 1 have indicated very large deuterium isotope effects, but have not been able to distinguish the primary isotope effect from the α-secondary effect. To address this question, singly deuterated linoleic acid was prepared, and enantiomerically resolved using the enzyme itself. Noncompetitive measurements of the primary deuterium isotope effect give a value of ca. 40 which is temperature-independent. The enthalpy of activation is low and isotope-independent, and there is a large isotope effect on the Arrhenius prefactor. A very large apparent secondary isotope effect (ca. 2.1) is measured with deuterium in the primary position, but a greatly reduced value (1.1) is observed with protium in the primary position. Mutagenesis of the active site leads to a significant reduction in k_{cat} and perturbed isotope effects, in particular, a secondary effect of 5.6 when deuterium is in the primary position. The anomalous secondary isotope effects are shown to arise from imperfect stereoselectivity of hydrogen abstraction which, for the mutant, is attributed to a combination of inverse substrate binding and increased flexibility at the reactive carbon. After correction, a very large primary (76−84) and small secondary (1.1−1.2) kinetic isotope effects are calculated for both mutant and wild-type enzymes. The weight of the evidence is taken to favor hydrogen tunneling as the primary mechanism of hydrogen transfer.

Lipoxygenases, a class of enzymes that catalyze the oxidization of the backbone of unsaturated fatty acids, are widely distributed in nature, occurring in species from cyanobacteria and yeasts through higher plants and mammals. A considerable degree of sequence identity is found among lipoxygenases, even for organisms as evolutionarily diverged as cyanobacteria and humans (*1*−*4*). The biological function of lipoxygenases is perhaps best established in mammalian tissues, where they catalyze the first few committed steps in the biosynthesis of a wide variety of eicosanoid inflammatory mediators, particularly the leukotrienes (*5*, *6*). They may also play a role in organelle membrane degradation (*7*). The physiological significance of lipoxygenases is less well established in plant tissue, where they have, however, been shown to be important in the biosynthesis of compounds involved in injury and infection response (e.g., plant hormones such as jasmonic acid, and compounds with direct antifungal properties) (*4*, *8*).

Although the biological significance of lipoxygenase is best understood in mammalian systems, fewer kinetic studies of these lipoxygenases have been carried out, a result of their complex behavior under steady state conditions and their relatively poor stability and availability. Plant lipoxygenases, by contrast, are easy to obtain, and are robust and kinetically tractable; for this reason, the majority of studies of lipoxygenase kinetics and mechanism have been carried out using soybean lipoxygenase 1 (SLO-1)[1] (*4*). Although the precise details of the chemical mechanism have not yet been elucidated, many features of the reaction catalyzed by SLO-1 are now well characterized. SLO-1 is a metalloenzyme, binding a single non-heme iron which cycles between the Fe(III) and Fe(II) oxidation states during the catalytic cycle (*9*). Recent crystal structures appear to rule out the presence of any other redox-active cofactors (*10*, *11*). The most widely accepted mechanism, depicted in Scheme 1, involves an initial concerted proton abstraction and one-electron oxidation of the substrate to produce a delocalized radical. This is then trapped by molecular oxygen to yield a peroxyl radical intermediate, which is subsequently reduced and protonated by the ferrous center and its water ligand, respectively. Both substrate and peroxyl radical species bound to enzyme have been observed by EPR, although the catalytic competence of the observed species has not been demonstrated (*12*−*14*). Steady state kinetic studies have demonstrated that oxygen only interacts with the enzyme following hydrogen abstraction from substrate and the reduction of the metal center, and that hydrogen abstraction is apparently irreversible (*15*).

There are a number of unusual aspects associated with SLO-1 and its mechanism which have been the subject of numerous studies. Lag periods are frequently observed during initial rate studies of the enzyme. These have been attributed to a requirement that the enzyme be oxidized from its resting

† This research was supported by National Institutes of Health Grant GM 25765. K.W.R. was supported by National Institutes of Health Postdoctoral Fellowship GM 17811.

* To whom correspondence should be addressed. J.P.K. is also in the Department of Molecular and Cell Biology at the University of California, Berkeley.

[1] Abbreviations: SLO-1, soybean lipoxygenase 1; HPOD, hydroperoxyoctadecadeinoic acid; HOD, hydroxyoctadecadeinoic acid.

10.1021/bi990834y CCC: $18.00 © 1999 American Chemical Society
Published on Web 08/27/1999

Scheme 1: Proposed Mechanism of the SLO-1 Reaction[a]

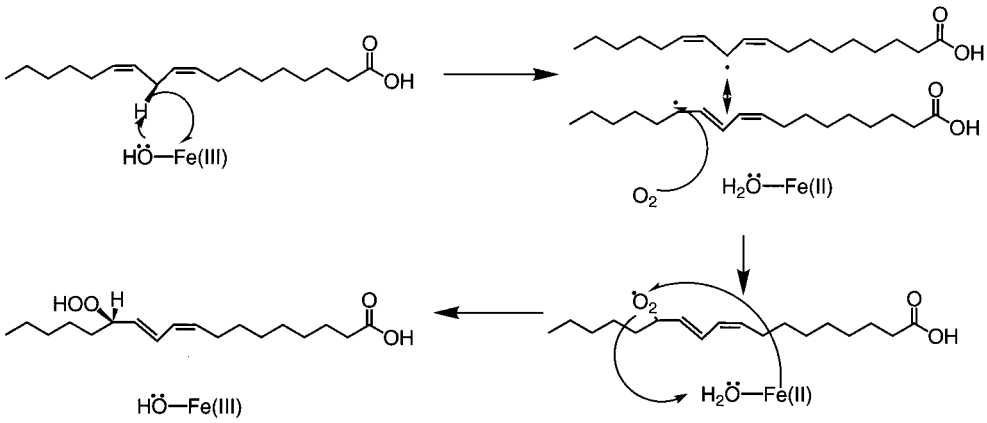

[a] The order of events after oxygen interaction with the substrate radical has not been established, and has been combined into one step for simplicity of presentation.

Fe(II) form to the Fe(III) form to achieve activity (*16*−*18*). Formation of the Fe(III) form is thought to be initiated by reaction with a small pool of autoxidized substrate, followed by a chain reaction in which the active pool of enzyme produces the lipid hydroperoxide product, which in turn oxidizes the remaining inactive enzyme. Another unusual feature is the role of oxygen in this reaction. A more typical mechanism for an oxygenase would begin with activation of oxygen by reduction, followed by attack of an activated oxygen species upon the substrate. For a metalloenzyme such as SLO-1, the iron center might perform this function by both binding molecular oxygen and providing the electrons needed for reduction. However, there is no evidence of oxygen binding to the iron center or of oxygen reduction, using either pre-steady state (*19*) or steady state techniques (*15*). Furthermore, since substrate hydrogen abstraction occurs before oxygen binding (*15*) and can occur in its absence (*20*), and reaction between the proposed radical intermediate and oxygen is spin-allowed, there would seem to be no reason for a metal−oxygen reaction to take place. This represents a unique mechanism of oxygen utilization for a metallooxygenase, presumably made possible by the extremely high reduction potential of the Fe(III) center in SLO-1 (*21*).

One particular feature of the enzyme which has attracted a great deal of interest is the observation of extremely large deuterium isotope effects, ranging from ca. 20 to 80, far larger than the value of 7−10 predicted with semiclassical theories (*20*, *22*, *23*). These observations have been made under a wide range of conditions, using both competitive and noncompetitive techniques and with a variety of isotopic substitution patterns. A number of possible causes for the size of this isotope effect have been considered. In some reactions, a branched reaction mechanism has been shown to lead to an observed isotope effect which is inflated beyond the semiclassical limit (*24*). However, only a single product has been observed for the SLO-1 reaction, and the pattern of isotope effects as a function of oxygen concentration is opposite of that expected if the large isotope effect were due to dissociation of a substrate-derived intermediate (*25*). An extremely large isotope effect is also observed for SLO-1 in a single-turnover experiment carried out under anaerobic conditions (*20*). The possibility of magnetic isotope effects in reactions generating radical intermediates has been discussed. This phenomenon has been observed in an enzymatic system, but does not appear to play a role in the lipoxygenase reaction (*23*, *26*). There are also a few enzymatic systems where the existence of a small pool of sites on the enzyme capable of receiving an abstracted hydrogen has led to the observation of inflated isotope effects (*27*). However, such an effect is ruled out with SLO-1 where large isotope effects are observed under steady state conditions using noncompetitive methods.

Hydrogen atom tunneling is another phenomenon which can give rise to hydrogen isotope effects that are larger than those permitted by semiclassical theory (*28*). Hydrogen tunneling, the quantum mechanical transfer of the hydrogen atom through rather than over a barrier, is perhaps most commonly associated with hydrogen transfers occurring at cryoscopic temperatures. Under such conditions, over-the-barrier processes, as predicted by classical transition state theory, cannot take place due to insufficient activation energy. However, in recent years a number of observations of tunneling behavior in enzymatic systems operating near room temperature have been made, suggesting that this may be a more common feature of enzymatic catalysis than previously thought (*29*−*31*). Observation of hydrogen tunneling within an enzymatic system is often difficult because steps other than the isotopically sensitive one may be partially rate-limiting, and a number of techniques have been developed to address this issue (*31*, *32*). With SLO-1, hydrogen abstraction has been shown to be significantly rate-limiting, allowing the issue of tunneling to be studied more directly.

One limitation of past studies of SLO-1 is that only substrates which are fully deuterated or dideuterated at the reactive C-11 position have been available (*20*, *22*, *23*). Using these materials, it has not been possible to distinguish the primary isotope effect from the α-secondary effect, leaving open the possibility that the α-secondary hydrogen may participate in the reaction in an unanticipated manner. In this work, we have prepared singly deuterated linoleic acid, which has allowed separate analysis of the 11-(*S*)-^{2}H and 11-(*R*)-^{2}H substrates by noncompetitive isotope effect studies. In addition, the behavior of the wild-type (WT) enzyme has been compared to that of a mutant designed to change the hydrogen transfer distance, and possibly favor an over-the-barrier transfer process (*33*). The net result of these studies is the demonstration that the very large isotope effects arise

from the cleaved primary position, with a very small contribution from secondary effects. Consideration of the properties of WT and mutant enzymes leads to the proposal of little or no classical component to C−H catalysis in the lipoxygenase reaction.

MATERIALS AND METHODS

Expression and Purification of SLO-1. Cultures of *Escherichia coli* BL21(DE3) cells transformed with the pT7-7/SLO-1 plasmid were grown as previously described (*34*). Cells from a 9 L fermentation mixture were harvested by centrifugation. The cell paste was suspended in 150 mL of sonication buffer [50 mM Tris-HCl (pH 7.5), 50 mM NaCl, 1 mM EDTA, 10% glycerol, 0.1% Tween 20, and 0.2 mM aminoethylbenzenesulfonyl fluoride (AEBSF)] and sonicated until OD(600) readings had declined to a constant value. $CaCl_2$ was added to the mixture at a final concentration of 50 mM, which was then incubated on ice for 15 min, followed by centrifugation at 27000*g* in an SS-34 rotor for 20 min. The supernatant was then brought to 33% of saturation with ammonium sulfate, stirred for 15 min, and centrifuged as described above. Again, the supernatant was retained, and was brought to 65% saturation of ammonium sulfate, and centrifuged. The precipitate from this step was frozen at −80 °C.

Ion-exchange chromatography began with dialysis of the redissolved protein into 20 mM imidazole-HCl buffer at pH 7.5. This was loaded on a large DE-52 column, and eluted with a salt gradient [20 mM imidazole-HCl (pH 7.5) and 0.5 M NaCl]. The fractions from this column with high activity were combined and concentrated on an Amicon concentrator, and then prepared for cation-exchange chromatography by dialysis into 25 mM MES and 10 mM NaCl (pH 5.8). This was followed by adsorption to a Mono-S column and elution with 25 mM MES and 0.25 M NaCl (pH 5.8). Following this procedure, specific activities of 160−180 μmol min^{-1} (mg of protein)$^{-1}$ were regularly achieved. These solutions were brought to 30% glycerol and frozen at −80 °C.

Synthesis of 11-(R,S)-[^{2}H]- and 11,11-[$^2H_2$]Linoleic Acid. We synthesized 11,11-[$^2H_2$]linoleic acid as described in the literature (*35*, *36*), although an alternate procedure was used to convert 2-octyn-1-ol to the corresponding bromide (*37*). The singly deuterated 11-(*R*,*S*)-[^{2}H]linoleic acid was prepared similarly, except that 2-octyn-1-ol was prepared by reduction of 2-octynal with sodium borodeuteride. The required 9-decynoic acid was synthesized from 9-decen-1-ol, the closest commercially available precursor.

HPLC Purification of Linoleic Acid. For all purifications, we used an Alltech Econosphere analytical (30 cm × 4.6 mm) C-18 column. Solvent A is 50% H_2O, 25% CH_3CN, 25% MeOH, and 0.05% trifluoroacetic acid. Solvent B is 10% H_2O, 65% CH_3CN, 25% MeOH, and 0.05% trifluoroacetic acid. The conditions used for the majority of purifications consisted of a linear gradient from 0 to 52% B over the course of 3 min, then a gradient from 52 to 72% B over the course of 12 min, a 1 min gradient from 72 to 100% B, 4 min at 100% B, and finally a 1 min gradient from 100 to 0% B. An isocratic elution at 60% B was used to repurify commercial linoleic acid; the resolution using this method was not sufficient to purify linoleic acid from synthetic mixtures. All traces were monitored at 210 and 234 nm; linoleic acid exhibited absorbance at only 210 nm. Purified linoleic acid was maintained under a nitrogen atmosphere. The retention times (t_R) for linoleic acid were 13.4 (gradient) and 6.0 min (isocratic). The t_R values for 13-hydroperoxy-9,11-(*Z*,*E*)-octadecadienoic acid were 11.0 (gradient) and 3.8 min (isocratic).

Enzymatic Resolution of 11-(R,S)-Deuteriolinoleic Acid. A linoleic acid stock solution (∼6 mg) was dissolved in 0.1 M borate buffer (pH 9.0) to a concentration of 60−100 μM. A 1 mL aliquot was removed and reacted with a large quantity of enzyme (60 nM), and the beginning and final absorbances at 234 nm were observed. The bulk of the solution (170 mL) was then incubated with enzyme (3 nM), and a 1 mL aliquot was removed and its 234 nm absorbance monitored. When the reaction was judged to be 55% complete, it was quenched by addition of 90 mL of 50% CH_3CN and 1% H_3PO_4. This mixture was then extracted with 3 × 50 mL of ethyl acetate, and the organic layers were combined, concentrated, and exchanged into methanol solution. The resulting solution was then purified by reverse-phase HPLC, as described above, to give ∼2.5 mg of 11-(*S*)-[^{2}H]linoleic acid with an enantiomeric excess (e.e.) of >95% (estimated from enzymatic kinetics).

Enzymatic Kinetics. The majority of enzyme assays were performed using a UV spectrophotometer to detect the increase at 234 nm associated with the conjugated double bonds found in the product but not the substrate (ϵ_M = 23 600). Most enzymatic assays took place in 0.1 M borate buffer (pH 9.0). Assays carried out at pH 8.0 used 0.1 M Tris-HCl; those carried out at pH 10 also used 0.1 M borate buffer. Linoleic acid concentrated stock solutions were made up in methanol, and diluted into buffer so that the total methanol content in the final assay was <1.5%. (Assays using methanol-free substrate demonstrated that methanol concentrations of up to 1.5% did not measurably perturb enzymatic rates.) Linoleic acid concentrations were accurately determined by allowing an assay to proceed to completion, and quantitating the 234 nm absorbance. Assays carried out at linoleic acid concentrations of ≥40 μM often exhibited a brief lag period, which was excluded for the determination of initial rates. Likewise, assays with 11-(*S*)-[^{2}H]linoleic acid exhibited a brief burst phase, associated with residual contamination by protonated material, which was also excluded from the rate determination. Assays were generally performed in a 1 mL volume, with substrate concentrations ranging from 1 to 80 μM. Higher substrate concentrations were avoided to prevent the formation of micelles or premicellar aggregates [the critical micelle concentration (CMC) for linoleic acid under these conditions has been measured at 200 μM] (*38*). For protonated linoleic acid, approximately 3 nM lipoxygenase was used for each assay; assays of the deuterated substrate used 10 times this quantity.

Mutagenesis. Plasmid DNA was purified from the expression strain using standard Qiagen midiprep protocols. Primers were synthesized for the mutations by incorporating an additional *Ase*I restriction site for screening purposes. Mutagenesis reactions used the Stratagene Quikchange kit standard protocols, using 125 ng of primers and 10 and 40 ng of template, with 10 min extension times for 16 thermal cycles. The initial transformation into XL1-Blue used SOC

medium (Gibco BRL) as the rescue medium for 1 h before plating on LB+amp plates. Five colonies were picked for each mutant and grown in 2 mL of superbroth with 100 μg/mL ampicillin. Qiagen minipreps were used to isolate plasmid DNA, and *Ase*I digests were run to screen for mutant DNA. Colonies exhibiting the appropriate digestion pattern were grown in larger culture, and plasmid DNA was isolated using the midiprep procedure. These five mutants were sequenced using the T7 Sequenase sequencing procedure, with alkaline lysis and a Mn(II) buffer to sequence close to the primer. Reading of the gel indicated that the sequences were exactly as expected for an ~100 bp stretch centered near the sites of mutation.

Mutant plasmids were transformed into electrocompetent BL21(DE3) cells using standard *E. coli* electroporation procedures, with 100 ng of plasmid DNA to 40 μL of cells. The rescue medium was SOC for 1 h, after which the cells were plated on LB+amp plates.

Preparation of 13-Hydroxy-9,11-(Z,E)-octadecadieneoic Acid (13-HOD). An 80 μM solution of 11-(*S*)-[^{2}H]linoleic acid in pH 9.0 buffer was incubated with enzyme and observed at 234 nm until the reaction was apparently complete. The reaction was quenched and the mixture extracted as described above for the enzymatic resolution. Trimethyl phosphite was added to the organic extracts at a final concentration of 1%, to reduce the hydroperoxide to alcohol, and the mixtures were incubated overnight. Following removal of the solvent, the mixture was redissolved in pH 9.0 buffer and the product purified using a C-18 SPE cartridge (Sep-Pak, Waters) eluted in fractions with acetonitrile/water. 13-Hydroxyoctadecadienoic acid (HOD) was identified in the fractions by analytical HPLC; these fractions were combined and dried, and the resultant material was submitted to negative ion FAB mass spectrometry. Note that under the conditions that were used, alcohol and hydroperoxide products cannot be distinguished by HPLC, but MS analysis demonstrated that reduction of the hydroperoxide was complete. The resultant peak patterns were deconvoluted into deuterium incorporation ratios by comparison with a control sample prepared using linoleic acid.

Regiochemistry Analysis. An 80 μM solution of 11-(*S*)-[^{2}H]linoleic acid was incubated in buffer with the relevant enzyme until the reaction seemed to be complete. Aliquots (100 μL) were analyzed by HPLC, with the solvents and column described above and using a gradient of 15 to 25% B over the course of 40 min. Retention times were near 26 min, with 13-hydroperoxyoctadecadienic acid (HPOD) eluting approximately 0.5 min earlier than 9-HPOD. Due to extensive overlap, peak areas were analyzed at 234 nm by fitting the combined peaks to a sum of two Gaussians with a nonlinear fit with fixed centers. With the WT enzyme at pH 10, an erroneously high value for the 9-HPOD component is measured due to peak tailing from the large 13-HPOD and was corrected.

RESULTS

Racemic 11-(R,S)-[^{2}H]Linoleic Acid. Enzymatic oxidation of the racemically deuterated linoleic acid followed biphasic kinetics, with the first phase being much faster than the second phase (Figure 1). Each of the two phases accounted for approximately 50% of the total oxidation seen when a reaction was allowed to proceed to its end point. SLO-1 is known at pH 9 to be stereospecific in the removal of protons from its substrate (*4*) such that the two phases can be assigned to oxidation of each of the two enantiomers of the racemically deuterated material. The extreme differences in the rates associated with each phase presumably arise from the large magnitude of the primary isotope effect. This difference in rate allows SLO-1 itself to be used as the basis of a kinetic resolution of the two enantiomers, providing 11-(*S*)-[^{2}H]-linoleic acid.

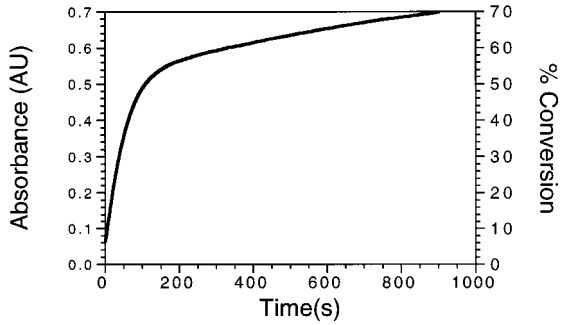

FIGURE 1: Rate of reaction of SLO-1 with 11-(*R,S*)-[^{2}H]linoleic acid, observed by UV absorbance at 234 nm. The reaction was carried out at 30 °C and pH 9.0 with 0.1 M borate, 40 μM linoleic acid, and 3 nM SLO-1.

Table 1: Apparent Isotope Effects on k_{cat} at 30 °C for WT and L546A SLO-1

enzyme	primary k_H/k_D	secondary k_H/k_D	primary k_H/k_D × secondary k_H/k_D
WT	40 ± 4	2.1 ± 0.2 1.1 ± 0.1 (H in primary position)	84 ± 8
L546A	16.6 ± 1.7	5.6 ± 0.6 1.2 ± 0.1 (H in primary position)	93 ± 9

Primary Isotope Effects. Using the stereospecifically deuterated linoleic acid, isotope effects could be measured for the single hydrogen atom being abstracted. Noncompetitive experiments carried out at 30 °C were used to measure k_H/k_D for k_{cat} of ca. 40 (Table 1). This is significantly lower than the values of ~80 observed previously for doubly deuterated substrates, but is still far outside the range predicted by semiclassical theories of 7−10. Effects on k_{cat}/K_M were very similar to those on k_{cat}, suggesting that under these conditions, substrate binding is not rate-limiting. Measurements made with both native and recombinant SLO gave identical results.

The predicted temperature dependence of an isotope effect varies significantly depending on whether the isotope effect has its origin in differential zero-point energies observed at the ground and transition states, as in semiclassical theories, or has its origin in differences in wave function penetration between reactant and product wells, as is the case for tunneling processes (*39*). Accordingly, noncompetitive isotope effect experiments in which linoleic acid and the 11-(*S*)-^{2}H material were compared were carried out over a wide temperature range (5−50 °C) (Figure 2). The measured k_H/k_D for k_{cat} is essentially temperature-independent over the entire observed range, as would be expected for a tunneling process. Semiclassical theories would predict a significant decrease in the isotope effect with increasing temperatures

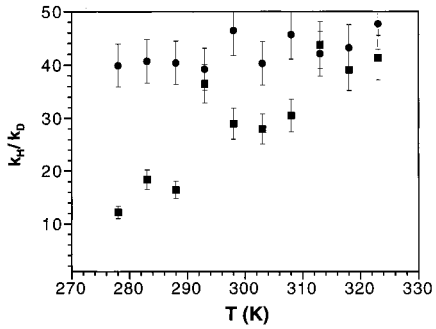

FIGURE 2: Apparent primary k_H/k_D at pH 9.0, by comparison of 11-(*S*)-[^{2}H]linoleic acid and linoleic acid. Effects are on k_{cat} (●) and k_{cat}/K_M (■).

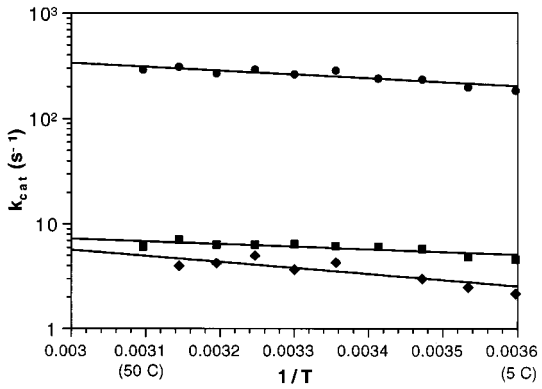

FIGURE 3: Arrhenius plots of k_{cat} for WT SLO-1, using linoleic acid (●), 11-(*S*)-[^{2}H]linoleic acid (■), and 11,11-[$^2H_2$]linoleic acid (◆). The results of the nonlinear fits for each data set are also shown.

(*39*). The observed temperature dependence of the isotope effect on k_{cat} differs from a previous result with the native enzyme, where the isotope effect was temperature-independent above 30 °C but decreased at lower temperatures, attributed to a change in the rate-determining step (*25*). The origin of this difference between native and recombinant enzymes is not currently known.

In contrast to the above result, the isotope effect upon k_{cat}/K_M does exhibit a pronounced temperature dependence, decreasing significantly at reduced temperatures. This is associated with a significant increase in the K_M for the protonated substrate at these temperatures; the K_M for the deuterated substrate actually decreases slightly as the temperature decreases. This discrepancy suggests that with the protonated substrate, substrate binding becomes rate-limiting at the lower temperatures; with the deuterated substrate, since the isotope effect upon k_{cat} is so large, hydrogen abstraction remains rate-limiting throughout the observed temperature range. A similar effect of rate limitation by substrate binding at reduced temperature was demonstrated earlier with native enzyme through the use of solvent viscosogens (*25*).

Another very distinctive feature of a pure quantum mechanical tunneling process through a static barrier is the absence of an energy of activation, as the barrier crossing is a temperature-independent process. The experiments carried out to measure the temperature dependence of the isotope effect also allow measurement of the Arrhenius parameters (Figure 3). With recombinant SLO-1, the observed $\Delta H^{\ddagger}$ values are very low for both protonated and deuterated substrates (Table 2) and similar to values seen previously with native SLO-1 (*20*). These values for $\Delta H^{\ddagger}$ are much lower than those observed for most chemical reactions, although they are clearly non-zero, indicating additional factors contributing to C−H activation (see the Discussion). As the activation energies are similar for protonated and deuterated substrates, the large isotope effects observed manifest themselves as an enormous isotope effect upon the Arrhenius prefactor, *A*. This is another sharp contrast with semiclassical theories, which predict that isotope effects on the Arrhenius prefactor will be close to unity (*39*).

Table 2: Enthalpies of Activation and Arrhenius Prefactor Isotope Effects for WT and L546A SLO-1

enzyme	substrate	$\Delta H^{\ddagger}$ (kcal/mol)	A_H/A_D
WT	linoleic acid	1.25 ± 0.2	−
WT	11-(*S*)-^{2}[H]linoleic acid	0.69 ± 0.2	110 ± 70
WT	11,11-[$^2H_2$]linoleic acid	2.4 ± 0.2	10 ± 7
L546A	linoleic acid	2.6 ± 0.4	−

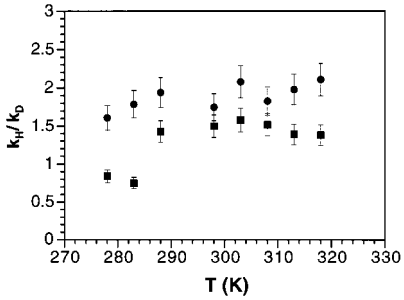

FIGURE 4: Apparent secondary k_H/k_D at pH 9.0, by comparison of 11-(*S*)-[^{2}H]linoleic acid and 11,11-[$^2H_2$]linoleic acid. Effects are that on k_{cat} (●) and k_{cat}/K_M (■).

Secondary Isotope Effects. With a source of stereospecifically deuterated linoleic acid, it is also possible to measure the α-secondary effect, i.e., the isotope effect from the hydrogen at C-11 which is not abstracted during the oxidation. This can most simply be done with a comparison between 11-(*S*)-[^{2}H]linoleic acid and the 11,11-$^2H_2$ substrate, where the secondary hydrogen atom is the only isotopic difference. These experiments were carried out in a nonconpetitive fashion, yielding a k_H/k_D of ca. 2 on k_{cat} in a nearly temperature-independent manner (Figure 4). This is consistent with earlier results, in which 11,11-[$^2H_2$]linoleic acid reacted ∼80 times slower than the protonated material, given the measurement of the primary effect at 40. Effects on k_{cat}/K_M were slightly lower, and appear to decrease somewhat as the temperature is reduced (Figure 4).

The secondary effect on k_{cat} is significantly larger than normal semiclassical predictions (1.0−1.25) (*40*, *41*). Secondary isotope effects as large as 2 have been observed, particularly in the cases of rotation around a double bond (*42*). However, in these cases the observed isotope effect has been dubbed "pseudo-primary", since a bending mode of the hydrogen atom disappears at the transition state, even though the bond itself is not broken. However, these cases do not seem to be immediately relevant to the lipoxygenase reaction. The large secondary effect would seem to arise as a result of the transfer process, as secondary effects on the adjacent carbons are much smaller (*43*).

Inflated secondary isotope effects have been observed in association with hydrogen atom tunneling when motions of the primary and secondary hydrogens are tightly coupled in the bond-breaking process (*31*). The increases in the second-

ary effect observed in such instances are typically modest, and are largest when tunneling is maximized. In the experiments described above with SLO-1, the secondary effect was measured with deuterium in the primary position. If coupled motion is responsible for the large secondary effect, then the secondary effect is predicted to be even larger when measured with protium in the primary position (since protium will undergo tunneling to a greater extent than deuterium).

Measurement of the α-secondary deuterium isotope effect with protium in the primary position would most simply be carried out by comparing the rate of oxidation of 11-(*R*)-[^{2}H]linoleic acid to linoleic acid. However, the enzymatic procedure used to resolve the two enantiomers of 11-[^{2}H]-linoleic acid specifically and irreversibly oxidizes this enantiomer. Accordingly, the racemic 11-(*R*,*S*)-[^{2}H]linoleic acid was used as a source of this material. The rate of oxidation of this material was compared to the rate observed with an equimolar mixture of linoleic acid and 11-(*S*)-[^{2}H]-linoleic acid, such that the total concentration of linoleic acid isomers and the concentration of 11-(*S*)-[^{2}H]linoleic acid were both the same in each case. The assumption was made that the 11-(*S*)-^{2}H material would have the same effect in each case and that, given the enormous primary isotope effect, this would be competition for binding with little contribution to the observed rate.

The results here are in sharp contrast to those observed when deuterium was in the primary position. The k_H/k_D measured at high substrate concentrations (thus indicative of the isotope effect on k_{cat}) was 1.1 ± 0.06. Although noncompetitive measurements are not highly accurate in this regime, the effect is clearly greatly reduced from that observed with deuterium in the primary position. This change is in the direction opposite from that expected if coupled motion of the secondary hydrogen to the tunneling primary hydrogen had inflated the secondary effect, suggesting that some other mechanism is responsible for the observed effects.

The simplest explanation would be that hydrogen abstraction is not fully rate-limiting when protium is being transferred and, thus, that the secondary isotope effect is not fully expressed in this case. When deuterium is transferred, given the large primary isotope effect, hydrogen transfer would become fully rate-limiting, and yield the full magnitude of the secondary effect. This type of behavior is well-precedented in multiple isotope effect measurements in other enzyme systems (*44*). However, there are two difficulties with such an explanation for SLO-1. One arises from the low $\Delta H^{\ddagger}$ values measured with both protium and deuterium in the primary position. Given an assumption that hydrogen abstraction is not fully rate-limiting for protium transfer, some other process must be partially rate-limiting; however, this process would also be required to have a similarly low $\Delta H^{\ddagger}$. This seems to be highly improbable, but cannot be ruled out. The other difficulty is that if hydrogen transfer were not fully rate-limiting for protium, the observed primary isotope effect is significantly smaller than the intrinsic effect. Given the discrepancy in the secondary effects, the intrinsic primary isotope effect would need to be ~300−400, an extremely large value that is unprecedented for isotope effects at room temperature. As with coupled motion, this does not seem to be a satisfactory explanation for the anomalous secondary isotope effects observed with SLO-1.

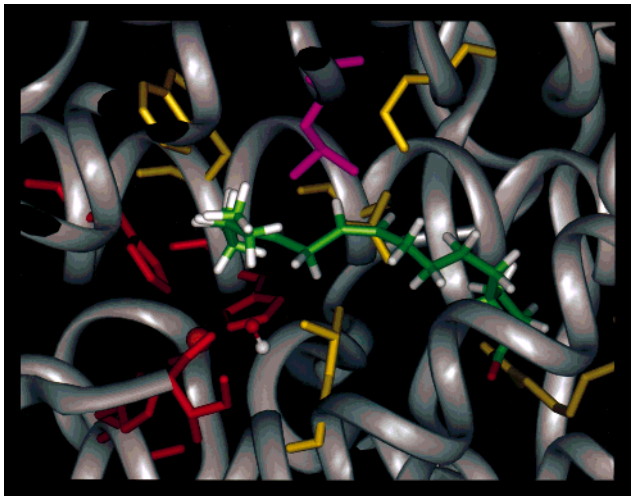

FIGURE 5: Crystal structure of the SLO-1 substrate binding pocket. Llinoleic acid (green) has been modeled into the site. Residues contacting the substrate are yellow, and the iron and its ligands are red. Leu546 is magenta.

Site-Directed Mutagenesis of SLO-1. Hydrogen tunneling is extremely sensitive to the distance over which hydrogen transfer occurs. This presents a striking contrast to a semiclassical transition state theory, in which there is no explicit dependence of the reaction rate upon transfer distance, only upon barrier height. To gain additional insight into the nature of the hydrogen tunneling process, site-directed mutagenesis was carried out on SLO-1, with the goal of changing the transfer distance. Molecular modeling of linoleic acid within the cavity in the crystal structure of SLO-1 (*10*) suggested that a small number of nonpolar residues might be important for substrate positioning near the iron center. One such residue, Leu546, was in relatively close proximity to C-11 of linoleic acid, the position of hydrogen abstraction (Figure 5). This residue is on the side of the substrate binding cavity opposite from the iron center believed to be responsible for hydrogen abstraction. Accordingly, it was mutated to alanine, as the decrease in size might allow the substrate to move further away from the iron center and thus slow hydrogen transfer dynamics. This might be expected to manifest itself as a reduction both in the overall rate and in the observed isotope effect (*33*, *45*).

SLO-1 L546A was expressed and purified using the same procedures established for WT SLO-1, and measurements of enzyme kinetics were taken. The most apparent effect of the mutation is the reduction of k_{cat} by about 250-fold, to 1 s^{-1}. The lag periods occasionally observed with the WT enzyme were much more pronounced with L546A, lasting up to several minutes under our conditions. The length of the lag period appeared to have a moderate temperature dependence. This is in contrast with the actual kinetics of catalysis, which exhibited a fairly low temperature dependence, similar to that of the WT enzyme (Table 2). Noncompetitive isotope effect measurements were carried out, and as before, large temperature-independent isotope effects were observed. The primary isotope effect observed with the L546A enzyme was ca. 17, significantly reduced from that observed with the WT enzyme (Table 1). However, there was a corresponding increase in the observed secondary effect, which was determined to be ca. 5.6. As a result, the product of the measured isotope effects (primary × second-

ary), which is also the isotope effect measured for linoleic acid versus 11,11-[$^2H_2$]linoleic acid, remained the same with the L546A mutant as for the WT.

Origin of Anomalous Secondary Isotope Effects. The extremely large secondary isotope effect observed with the L546A mutant is far larger than can be explained conventionally, and is actually of the size normally expected for primary isotope effects. This suggests that the magnitude of this effect may be artifactual in origin, reflecting a contribution from the large primary isotope effect in addition to the true secondary effect. This is further supported by the observation that the increase in the secondary isotope effect observed with the L546A mutation is matched by the apparent decrease in the primary effect. These matched imbalances could be explained by some factor which affects the apparent rate of reaction of 11-(*S*)-[^{2}H]linoleic acid without affecting the rates of reaction of symmetrically substituted molecules. This could also explain the anomalous secondary isotope effects observed with the WT enzyme; both the large isotope effect observed with deuterium in the primary position and the small effect observed with protium in the primary position would be predicted if this were the case.

What might affect the rate of reaction of the asymmetrically deuterated molecule in a selective manner? Although literature reports that the SLO-1 hydrogen abstraction is stereoselective under the conditions of these experiments (*4*), less than complete stereoselectivity might explain the observed phenomena. In this event, the observed oxidation rate of 11-(*S*)-[^{2}H]linoleic acid would be faster than predicted by the intrinsic primary isotope effect, since some proportion of the observed rate would be due to abstraction of the 11-(*R*)-proton and, thus, not subject to the large primary isotope effect. The result would be an apparent decrease in the primary isotope effect. By contrast, when 11,11-[$^2H_2$]linoleic acid is subjected to enzymatic oxidation, no such increase in rate would be possible, since the enzyme can only abstract deuterium. To formulate the observations in a more quantitative manner, each of the independently observed isotope effects is represented below with the appropriate substitutions:

$$\text{primary}\left(\frac{k_H}{k_D}\right)_{obs} = \frac{1+L}{p^{-1}+Ls^{-1}} \quad (1)$$

$$\text{secondary}\left(\frac{k_H}{k_D}\right)_{obs} = \frac{1+L}{s^{-1}+Lp^{-1}} \quad (2)$$

$$\text{primary}\left(\frac{k_H}{k_D}\right)_{obs} \times \text{secondary}\left(\frac{k_H}{k_D}\right)_{obs} = ps \quad (3)$$

where *p* and *s* represent the intrinsic primary and secondary isotope effects, respectively, while *L* represents the ratio of the rate for the 11-(*R*) to the rate for the 11-(*S*) position.

The above formulation yields three equations with three unknowns, which can be solved to give both the intrinsic isotope effects and the relative rate of reaction at the 11-(*R*) position compared to that at the 11-(*S*) position for unsubstituted linoleic acid. Although multiple roots are found, only one physically meaningful solution exists. As seen in Table 3, the intrinsic isotope effects calculated for both WT SLO-1 and the L546A mutant are essentially identical. In either case, the primary isotope effect is extremely large, while the secondary isotope effect is small and within the range normally expected. The significant difference between the WT and mutant enzymes, however, is in the relative rates of 11-(*R*) reactivity, which is increased by a factor of 5 for the mutant (Table 4).

Table 3: Intrinsic Isotope Effects for WT and L546A Enzymes

enzyme	primary k_H/k_D	secondary k_H/k_D
WT	76 ± 8	1.1 ± 0.1
L546A	78 ± 8	1.2 ± 0.1

Table 4: Percent Reaction at the 11-(*S*) and 11-(*R*) Positions of the Substrate with WT and L546A SLO-1

enzyme	% 11-(*S*) reaction	% 11-(*R*) reaction
Predicted Reaction with Linoleic Acid[a]		
WT	99	1
L546A	95	5
Predicted Reaction with 11-(*S*)-[^{2}H]Linoleic Acid[b]		
WT	62	38
L546A	23	77
Observed Reaction with 11-(*S*)-[^{2}H]Linoleic Acid[c]		
WT	55 ± 5	45 ± 5
L546A	27 ± 5	73 ± 5

[a] Calculated from eqs 1−3. See the text. [b] Calculated from the intrinsic isotope effects and *L* using the relation $(p^{-1})/(p^{-1} + Ls^{-1})$. [c] From FAB-MS analysis of reduced, 13-HOD products.

Although the inherent rates of reactivity at the 11-(*R*) position are very low, when an 11-(*S*) deuterated substrate is oxidized, the large primary isotope effect should substantially change the relative rates of reaction. Using the model described above, relative reaction rates for the 11-(*R*) and 11-(*S*) positions with an 11-(*S*)-^{2}H substrate and either the WT or L546A enzyme can be calculated (Table 4). In this case, reaction at the 11-(*R*) position is predicted to be much more favorable than that with the unlabeled linoleic acid; in the case of the L546A mutant, the 11-(*R*) reaction occurs a majority of the time. This suggests how this model may be tested, as reaction at each of the two positions results in the removal of a different isotope of hydrogen. Accordingly, the oxidized product will contain a mixture of hydrogen and deuterium atoms in a corresponding ratio, and these can be measured by mass spectrometry. As shown in Table 4, the observed product isotope ratios closely match the predictions, and clearly demonstrate the incomplete stereoselectivity of hydrogen abstraction, leading to the observed anomalous isotope effects.

What is the cause of these changes in the stereochemistry of hydrogen abstraction? It might simply arise from poor discrimination between the two hydrogens at C-11 within a single binding mode (pathway B in Scheme 2). A second possibility is that the substrate binds to the active site in an inverted orientation, reversing both the stereochemistry of hydrogen abstraction and the regiochemistry of product formation (pathway C in Scheme 2). An inverted binding orientation has been observed for SLO-1 at low pH, resulting in an increase in the level of formation of 9-HPOD in a highly pH-dependent manner (*46*). Although this has not been observed to be a significant factor at pH ≥8.0, it becomes difficult to determine low levels of enzymatic 9-HPOD formation and to distinguish it from autoxidation

Scheme 2: Alternative Reaction Pathways for Reaction of SLO-1 with 11-(*S*)-[^{2}H]Linoleic Acid[a]

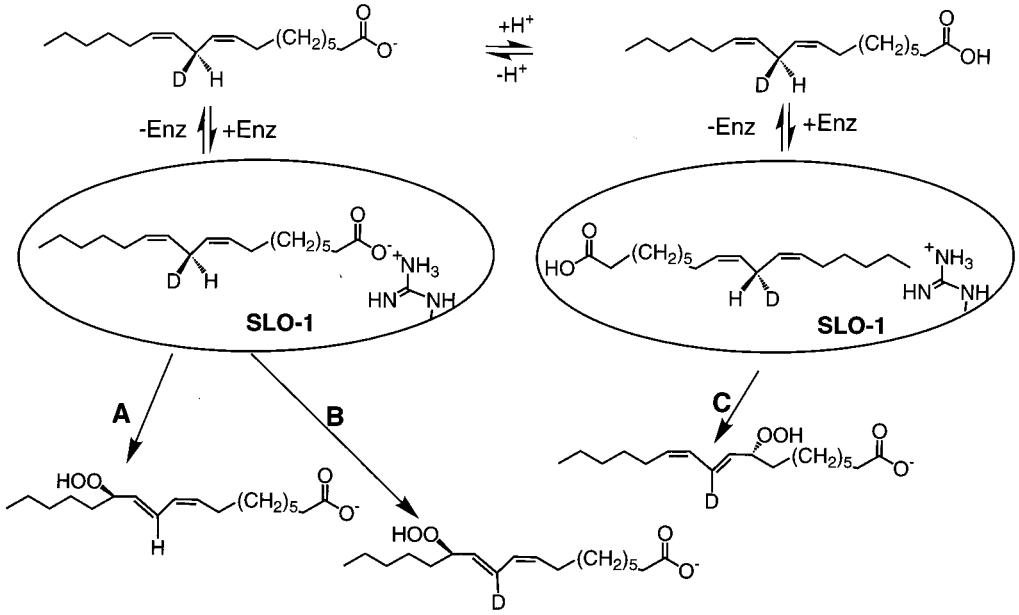

[a] Pathway A is the predominant reaction pathway with a non-deuterated substrate.

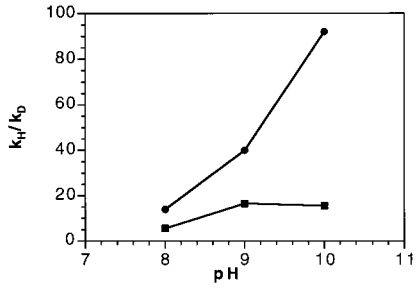

FIGURE 6: pH dependence of the primary isotope effect measured with 11-(*S*)-[^{2}H]linoleic acid for the WT (●) and L546A (■) enzymes.

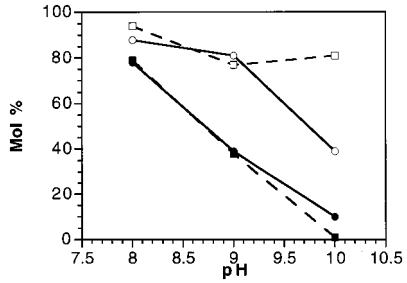

FIGURE 7: Comparison of the mole % reaction of 11-(*R*) abstraction (squares) (calculated from isotope effects; see Table 4) with the observed mole % of 9-HPOD products (circles). Black symbols represent the results with the WT enzyme, and white symbols represent the results with the L546A mutant.

products and semi-enzymatic product formed from loss of an intermediate product radical into solution (*47*). However, measurement of the apparent primary isotope effect using the singly deuterated substrate should be very sensitive to reaction from an inverted binding mode. This effect was measured over the pH range of 8−10 for both WT and L546A enzymes (Figure 6). Because the isotope effect measured with a dideuterated substrate was essentially independent of pH over this range (*25*), variations here directly reflect changes in the stereochemistry of hydrogen abstraction. The effect observed with the WT enzyme exhibits a very strong dependence on pH, decreasing substantially at pH 8.0, but increasing at pH 10.0 to nearly the full value observed with a dideuterated substrate. The trend suggests that essentially all the 11-(*R*) abstraction observed with the WT enzyme occurs as a result of inverse substrate orientation, and that this process becomes negligible at pH 10. This interpretation is confirmed by direct measurement of the 9-HPOD content (Figure 7). The 9-HPOD content closely matches the calculated extent of 11-(*R*) abstraction, demonstrating that 11-(*R*) abstraction only occurs with the inverse substrate orientation. In contrast, although the L546A enzyme does exhibit a reduction in the primary isotope effect at pH 8.0, at pH 10.0 the isotope effect is unchanged from that observed at pH 9.0 (Figure 6). The data shown in Figure 7 confirm that with the L546A mutant, inverse substrate orientation is important to 11-(*R*) abstraction at lower pH values, and that the mutant reacts more readily in this orientation than the WT enzyme. However, the data also demonstrate that at pH 10, there is a significant contribution to 11-(*R*) abstraction, which proceeds directly without inverse substrate orientation.

DISCUSSION

Having prepared a chirally labeled linoleic acid with a single deuterium and measured noncompetitive isotope effects with SLO-1 under a variety of conditions, we can draw a number of conclusions about the process of hydrogen transfer. Three key pieces of data point to the involvement of a nonclassical transfer.

The first such piece of data is the size of the primary isotope effect. Now that the exact size of this effect has been established, it is clear that it is far larger than can be explained by semiclassical theories of isotope effects. Thus far, investigations of a number of other possible causes of anomalously large isotope effects have not yielded an explanation for the large isotope effects observed with SLO-1. Most theoretical studies of tunneling in enzymes have focused on cases where the degree of hydrogen tunneling is modest, and can be addressed using the Bell correction to

the semiclassical rates (*28*). This correction is not realistically able to produce the magnitude of deviation from the semiclassical predictions of isotope effects observed here. Recent theoretical work with this enzyme has yielded an isotope effect for a purely quantum mechanical mechanism of more than 10^5, and required an extreme inverse isotope effect along the classical reaction coordinate to bring the calculated net isotope effect into agreement with the observed value (*48*). However, the extremely tight nature of the proposed transition state (inducing an inverse isotope effect of more than 10^3) does not seem to be physically meaningful. A theory of tunneling in which tunneling transfer is coupled to a vibrational mode which results in enhanced tunneling rates may be able to reproduce some of these phenomena, but a detailed application to SLO-1 has not yet been presented (*49*).

The temperature independence of the isotope effect is another key piece of evidence which favors hydrogen tunneling. Semiclassical theories predict that isotope effects arise from isotopic differences in zero-point energy in the ground state energy well and in the transition state, leading to differences in activation energy for each isotopically substituted compound (*50*). The observed isotope effect should have a pronounced temperature dependence, as the isotopic differences in activation energy will disappear at the limit of infinite temperature. For a purely tunneling mechanism, however, a very different result is predicted. For ground state tunneling through a static barrier, there is no energy of activation associated with the transfer itself. The isotope effect on rate should be temperature-independent, arising from different properties of the nuclear wave functions (*39*). Accordingly, the isotope effect will appear in the Arrhenius prefactor, as is observed for SLO-1. There is no consistent difference in the activation energies depending upon the isotope in the primary position, and there is certainly not enough to account for the magnitude of the primary isotope effect (Table 2). Furthermore, extremely large isotope effects on the Arrhenius prefactor are observed. All of these phenomena are most consistent with hydrogen tunneling as the mechanism of hydrogen transfer.

The low enthalpy of activation observed for this reaction provides further support for a hydrogen tunneling mechanism. The enthalpy of activation observed for these reactions, 1−2 kcal/mol for the WT (Table 2), is extremely low in comparison with those of other enzymatic reactions (*31*). With SLO-1, it is clear that hydrogen abstraction has to be significantly rate-limiting, on the basis of the magnitude of the isotope effect and its temperature independence over a range from 5 to 50 °C. A rate-limiting hydrogen abstraction with a low enthalpy of activation is unprecedented in the absence of hydrogen tunneling; typical hydrogen abstractions exhibit an enthalpy of activation of ≥8−15 kcal/mol (*31*). Furthermore, with such a low enthalpy of activation, it may seem surprising that this step is rate-limiting; the result suggests an enormous entropic barrier to reaction, which in classical terms is surprising for a state in which all reactants are already bound. However, such an apparent barrier to reaction can be provided in a ground state hydrogen tunneling model. The tunneling process itself should exhibit no enthalpy of activation, but may exhibit significant entropic barriers which are dependent on the cross-sectional terms of the tunneling function. One of the tunneling models described above, in which hydrogen and electron tunneling are coupled processes, assumes no enthalpy of reaction (*48*). However, in this model it is difficult to account for the small, but non-zero enthalpy of reaction that is actually observed. This is perhaps better accounted for in the other model that is described, which couples productive tunneling to a vibrational mode of the enzyme/substrate system (*49*). Here the observed enthalpy of activation encompasses both the enthalpy of activation of the vibrational mode and the thermodynamic enthalpy of reaction. When these two enthalpies are closely balanced, a very low overall enthalpy of activation, as is observed with SLO-1, could be achieved.

Initially, the anomalous observations of large secondary isotope effects were quite surprising, and were attributed to some unappreciated aspect of the unusual hydrogen transfer. The realization that imperfect stereoselectivity of hydrogen abstraction might cause such an effect made a substantial contribution to the understanding of both primary and secondary isotope effects in this reaction. The degree of stereo- and regioselectivity that is normally observed under these conditions is quite high (Table 4), and it is not surprising that other techniques had been unable to distinguish the small deviations from that arising from other mechanisms. However, when coupled with the enormous primary isotope effect, even a very low rate of abstraction from the 11-(*R*) position results in a significant perturbation of rate and, hence, of the apparent isotope effects. A more direct observation of the abstracted hydrogen, such as would be possible with a tritium-labeled substrate, could have avoided this confusion, but might itself be prone to artifactual results, as has been observed in other systems (*27*). The results presented herein for SLO-1 demonstrate that isotope effects can be a very sensitive probe of the regio- and stereochemistry of enzymatic oxidation.

With the value of the actual α-secondary isotope effect having been established, it appears to be normal in size, and consistent with a bond hybridization change at the reactive carbon (*45*, *46*). However, how this interpretation applies to a system where hydrogen tunneling is extensive and the transition state is never actually crossed is not clear, and current hydrogen tunneling theories do not address secondary isotope effects. Furthermore, even the small magnitude of this effect might be considered unusual, as inflated α-secondary isotope effects have been observed in several enzymatic systems which are characterized by both hydrogen tunneling and a coupling of motion between the α-secondary and primary hydrogens (*29*, *32*). Furthermore, in systems of this type, it does not appear that tunneling is as extensive as is observed for SLO-1, leading to the question of why such an inflation of the secondary isotope effect is not seen with SLO-1. One simple explanation would be that the α-secondary hydrogen does not undergo a significant degree of coupled motion during the hydrogen transfer process, a claim which may be difficult to address without a deeper understanding of the motions of the substrate and hydrogen acceptor during the reaction. As the noncompetitive experiments used in this paper are relatively inaccurate at discerning small isotope effects, further interpretation should await a more well-defined number obtained via a competitive technique.

In addition to providing a key insight into understanding the secondary isotope effects, the kinetic results from the

L546A mutant also throw additional light on the nature of hydrogen tunneling within SLO-1. Although there is a substantial reduction in the overall rate of reaction, the isotope effects remain the same (Table 3). These results suggest that over-the-barrier hydrogen transfer must be extremely slow within this active site since, despite the substantial reduction in the hydrogen abstraction rate, there are no signs that this process is contributing to that rate in L546A. This indicates that the potential surface for the SLO-1 reaction has some very peculiar features. How does the mutation affect tunneling? The introduction of direct 11-(*R*) abstraction (pathway B, Scheme 2) shows that this mutation has significantly affected the relative position of the substrate hydrogens and the hydrogen acceptor. It is possible that there is a simple increase in the distance between the substrate and the acceptor, in keeping with our initial hypothesis. However, in the absence of semiclassical hydrogen transfer, an increase in the tunneling distance might be expected to increase the isotope effect, which is not observed. An alternative explanation might be found within the dynamically enhanced tunneling model (*49*). If tunneling only takes place from certain enzyme or substrate configurations, it may be that tunneling in the L546A protein exhibits identical isotope effects because it is occurring from the same configurations and with the same exciting vibrational mode (*51*). The increased energy required to achieve this exciting vibrational mode may be reflected in the increase in $\Delta H^{\ddagger}$ from 1.25 ± 0.2 to 2.6 ± 0.4 kcal/mol for WT and L546A, respectively (Table 2). Additionally, the mutation might have made it entropically more difficult for the enzyme to achieve the critical configuration(s) required for tunneling, thereby accounting for the substantial reduction in the overall rate that was observed.

In many other enzymatic systems, definitive evidence for hydrogen tunneling behavior has rested upon fairly subtle signatures, such as the ratios of deuterium and tritium isotope effects (*29*, *32*). In part, this is due to the presence of isotopically insensitive rate-limiting steps within the mechanisms of these enzymes. A further contributing factor is the participation of both hydrogen tunneling and over-the-barrier transfers to the same process. In this context, work with SLO-1 appears to offer a distinct opportunity to examine enzymatic hydrogen tunneling in the absence of competing semiclassical processes. Future work with tritium isotope effects may help further define the nature of the transfer, extend the available experimental data on isotope effect ratios into a system with more extensive hydrogen tunneling, and provide a tool for evaluation of tunneling theories. Defining systems in which tunneling takes place and can be readily examined is essential for developing a greater understanding of the tunneling process itself, the means by which an enzyme active site catalyzes tunneling, and why certain enzymes have evolved to favor this mechanism of hydrogen transfer.

APPENDIX

Derivation of Equations 1−3. The core assumption is that the net rate of reaction by SLO-1 with any substrate is the sum of the rates of reaction at the 11-(*S*) and the 11-(*R*) position. The rate of reaction at the 11-(*R*) position is a minor component. So, for linoleic acid, the rate expression is as follows, where, as in eqs 1 and 2, *L* represents the ratio of the rate of reaction at the 11-(*R*) position to that at the 11-(*S*) position.

$$k = r + Lr \tag{4}$$

In eqs 4−7, *r* is an arbitrary variable, representing the inherent rate of oxidation at the 11-(*S*) position with linoleic acid.

Deuteration at the 11-(*S*) position imposes the primary isotope effect upon the 11-(*S*) reaction, and the secondary isotope effect upon the 11-(*R*) reaction. This gives rise to the following expression:

$$k_D = \frac{r}{p} + L\frac{r}{s} \tag{5}$$

This can be combined with eq 4 to give eq 1, which gives the observed primary isotope effect for the 11-(*S*) deuterated substrate.

A similar principle can be followed to give the expression for 11-(*R*) deuteration:

$$k_D = \frac{r}{s} + L\frac{r}{p} \tag{6}$$

And similarly, in combination with eq 4, eq 2 for the observed secondary isotope effect can be derived.

Finally, with the doubly deuterated substrate, both secondary and primary isotope effects contribute, regardless of the position of reaction:

$$k_D = \frac{r}{ps} + L\frac{r}{ps} \tag{7}$$

This, in turn, gives rise to eq 3.

SUPPORTING INFORMATION AVAILABLE

Descriptions of the syntheses of 11-(*R*,*S*)-[^{2}H]linoleic acid and 11,11-[$^2H_2$]linoleic acid. This material is available free of charge via the Internet at http://pubs.acs.org.

REFERENCES

1. Siedow, J. N. (1991) *Annu. Rev. Plant Physiol. Mol. Biol. 42*, 145−188.
2. Sigal, E. (1991) *Am. J. Physiol. 260*, L13−L28.
3. Nelson, M. J., and Seitz, S. P. (1994) *Curr. Opin. Struct. Biol. 4*, 878−884.
4. Gardner, H. W. (1991) *Biochim. Biophys. Acta 1084*, 221−239.
5. Samuelsson, B., Dahlén, S.-E., Lindgren, J. Å., Rouzer, C. A., and Serhan, C. N. (1987) *Science 237*, 1171−1176.
6. Ford-Hutchinson, A. W., Gresser, M., and Young, R. N. (1994) *Annu. Rev. Biochem. 63*, 383−417.
7. van Leyen, K., Duvoisin, R. M., Engelhardt, H., and Wiedmann, M. (1998) *Nature 395*, 392−395.
8. Vick, B. A., and Zimmerman, D. C. (1984) *Plant Physiol. 75*, 458−461.
9. Funk, M. O. J., Carroll, R. T., Thompson, J. F., Sands, R. H., and Dunham, W. R. (1990) *J. Am. Chem. Soc. 112*, 5375−5376.
10. Minor, W., Steczko, J., Stec, B., Otwinowski, Z., Bolin, J. T., Walter, R., and Axelrod, B. (1996) *Biochemistry 35*, 10867−10701.
11. Boyington, J. C., Gaffney, B. J., and Amzel, L. M. (1993) *Science 260*, 1482−1486.
12. Nelson, M. J., and Cowling, R. A. (1990) *J. Am. Chem. Soc. 112*, 2820−2821.

13. Nelson, M. J., Seitz, S. P., and Cowling, R. A. (1990) *Biochemistry 29*, 6897−6903.
14. Nelson, M. J., Cowling, R. A., and Seitz, S. P. (1994) *Biochemistry 33*, 4966−4973.
15. Glickman, M. H., and Klinman, J. P. (1996) *Biochemistry 35*, 12882−12892.
16. Schilstra, M. J., Veldink, G. A., Verhagen, J., and Vliegenthart, J. F. G. (1992) *Biochemistry 31*, 7692−7699.
17. Schilstra, M. J., Veldink, G. A., and Vliegenthart, J. F. G. (1993) *Biochemistry 32*, 7686−7691.
18. Schilstra, M. J., Veldink, G. A., and Vliegenthart, J. F. G. (1994) *Biochemistry 33*, 3974−3979.
19. Petersson, L., Slappendel, S., and Vliegenthart, J. F. G. (1985) *Biochim. Biophys. Acta 828*, 81−85.
20. Jonsson, T., Glickman, M. H., Sun, S., and Klinman, J. P. (1996) *J. Am. Chem. Soc. 118*, 10319−10320.
21. Nelson, M. J. (1988) *Biochemistry 27*, 4273−4278.
22. Glickman, M. H., Wiseman, J. S., and Klinman, J. P. (1994) *J. Am. Chem. Soc. 116*, 793−794.
23. Hwang, C.-C., and Grissom, C. B. (1994) *J. Am. Chem. Soc. 116*, 795−796.
24. Thibblin, A. (1988) *J. Phys. Org. Chem. 1*, 161−167.
25. Glickman, M. H., and Klinman, J. P. (1995) *Biochemistry 34*, 14077−14092.
26. Harkins, T. T., and Grissom, C. B. (1994) *Science 263*, 958−960.
27. O'Brien, R. J., Fox, J. A., Kopczynski, M. G., and Babior, B. M. (1985) *J. Biol. Chem. 260*, 16131−16136.
28. Bell, R. P. (1980) *The Tunnel Effect in Chemistry*, Chapman and Hall, New York.
29. Cha, Y., Murray, C. J., and Klinman, J. P. (1989) *Science 243*, 1325−1330.
30. Bahnson, B. J., Park, D.-H., Kim, K., Plapp, B. V., and Klinman, J. P. (1993) *Biochemistry 32*, 5503.
31. Kohen, A., and Klinman, J. P. (1998) *Acc. Chem. Res. 31*, 397−404.
32. Bahnson, B. J., and Klinman, J. P. (1995) *Methods Enzymol. 249*, 373−397.
33. Bahnson, B. J., Colby, T. D., Chin, J. K., Goldstein, B. M., and Klinman, J. P. (1997) *Proc. Natl. Acad. Sci. U.S.A. 94*, 12797−12802.
34. Steczko, J., Donoho, G. A., Dixon, J. E., Sugimoto, T., and Axelrod, B. (1991) *Protein Expression Purif. 2*, 221−227.
35. Osbond, J. M., Philpott, P. G., and Wickens, J. C. (1961) *J. Chem. Soc.*, 2779−2787.
36. Tucker, W. P., Tove, S. B., and Kepler, C. R. (1970) *J. Labelled Compd. 8*, 11−15.
37. Corey, E. J., Kim, C. U., and Takeda, M. (1972) *Tetrahedron Lett. 42*, 4339−4342.
38. Glickman, M. (1994) Mechanistic Studies of Soybean Lipoxygenase, Ph.D. Thesis, University of California, Berkeley, CA.
39. Benderskii, V. A., Makarov, D. E., and Wight, C. A. (1994) *Adv. Chem. Phys. 88*, 151−207.
40. Gajewski, J. J., Olson, L. P., and Tupper, K. J. (1993) *J. Am. Chem. Soc. 115*, 4548−4553.
41. Houk, K. N., Gustafson, S. M., and Black, K. A. (1992) *J. Am. Chem. Soc. 114*, 8565−8572.
42. Caldwell, R. A., Misawa, H., Healy, E. F., and Dewar, M. J. S. (1987) *J. Am. Chem. Soc. 109*, 6869−6870.
43. Wiseman, J. S. (1989) *Biochemistry 28*, 2106−2111.
44. Cleland, W. W. (1991) in *Enzyme Mechanism from Isotope Effects* (Cook, P. F., Ed.) pp 247−265, CRC Press, Boca Raton, FL.
45. Colby, T. D., Bahnson, B. J., Chin, J. K., Klinman, J. P., and Goldstein, B. M. (1998) *Biochemistry 37*, 9295−9304.
46. Gardner, H. W. (1989) *Biochim. Biophys. Acta 1001*, 274−281.
47. Berry, H., Dèbat, H., and Larreta Garde, V. (1998) *J. Biol. Chem. 273*, 2769−2776.
48. Moiseyev, N., Rucker, J., and Glickman, M. H. (1997) *J. Am. Chem. Soc. 119*, 3853−3860.
49. Antoniou, D., and Schwartz, S. D. (1997) *Proc. Natl. Acad. Sci. U.S.A. 94*, 12360−12365.
50. Melander, L., and Saunders, W. H. (1987) *Reaction rates of isotopic molecules*, Krieger, Malabar, FL.
51. Kohen, A., and Klinman, J. P. (1999) *Chem. Biol.* (in press).

BI990834Y